RSC Advances

PAPER

Cite this: *RSC Adv.*, 2021, **11**, 37575

A TiO_2 composite with graphitic carbon nitride as a photocatalyst for biodiesel production from waste cooking oil

Mahrukh Khan,[a] Humera Farah,[a] Naseem Iqbal,*[b] Tayyaba Noor,[c] M. Zain Bin Amjad[b] and Syeda Sidrah Ejaz Bukhari[a]

Received 22nd October 2021
Accepted 16th November 2021

DOI: 10.1039/d1ra07796a

rsc.li/rsc-advances

Semiconductor-based photocatalysts have attracted a lot of interest due to their environmental friendliness and high stability. Waste cooking oil can be converted to biodiesel by the process of transesterification. A TiO_2/g-C_3N_4 combination was prepared by using a wet impregnation process. The photocatalyst was analyzed by X-Ray Diffraction (XRD), Scanning Electron Microscopy (SEM), Energy Dispersive X-Ray spectroscopy (EDX), Thermogravimetric analysis (TGA), and Ultraviolet-visible spectroscopy (UV-vis). For effective transesterification, WCO was collected and acid-esterified to reduce the FFA concentration (below 3%). For the transesterification reaction, esterified WCO was used and the reactions were carried out under solar irradiation at 60 °C with an oil to methanol ratio of 1 : 9 and stirred for 1 hour, using different TiO_2/g-C_3N_4 catalysts (10, 20 & 30%) with different catalyst concentrations of 1%, 2% and 3%. The results showed that TiO_2/20% g-C_3N_4 with 2% catalyst concentration gives the highest yield of biodiesel production (89.5%) as compared to other catalyst concentrations used. In addition to (FTIR), additional fuel characteristics such as density, viscosity, flashpoint, acid value, and pH were tested to determine the quality of the generated biodiesel and were found to comply with fuel standards. With high stability and good catalytic activity, the synthesized composite TiO_2/g-C_3N_4 is a viable option for producing biodiesel from WCO.

1. Introduction

In the current energy scenario, fossil-based fuels are being used to meet the majority of energy demand. Due to their environmental impact, these energy supplies will cause an energy crisis in the next several decades if they are used excessively.[1,2] Furthermore, the scarcity of petroleum sources and rising oil costs have increased the demand to find a clean, environmentally friendly alternative fuel.[3,4] Biodiesel is gaining more acceptance in the energy sector as a unique fuel due to its availability, eco-friendly, non-toxicity, and most importantly its production from renewable feedstocks.[5,6] Biodiesel is composed of fatty acid methyl ester that is formed when oils are transesterified with alcohol in the presence of a catalyst.[7] Several food oils can be used to produce biodiesel (castor oil, olive oil, and mustard oil) as well as non-consumable feedstock oils (Jatropha oil, Jojoba oil).[8–10] Consumption of edibles oils has a food supply problem whereas crops that produce non-edible oils need additional farmland, limiting their utilization on a big scale. Other raw material sources must be identified to manufacture low-cost biodiesel.[11]

When we cook meals, we consume a lot of vegetable oil, which may be used to produce biodiesel.[12] As a result of its lower solubility in water, disposing of WCO in open areas will harm the environment. Hence the renewable energy research targets this oil used for biodiesel production being a cheap feedstock.[13,14] A transesterification reaction was used to produce biodiesel in the presence of a catalyst (alkaline, acidic, and photocatalyst). WCO requires pretreatment before transesterification, constant exposure to heat during frying causes oxidation as well as a rise in the free fatty acid (FFA) concentration which increases the time and energy required for transesterification.[15] For this reason, WCO for biodiesel production needs to be purified to minimize the amount of FFA. The WCO was collected from restaurants and the waste oil was firstly esterified before transesterification. Sulphuric acid was able to catalyze esterification in the presence of alcohol and WCO and after that, the esterified oil is then reacted with a catalyst to produce fatty acid methyl ester (FAME).[16] There is a growing interest in semiconductor photocatalysis because of its possible applications in fields such as nature, solar energy, and renewable energy, as well as medicine. A variety of semiconductors, including ZnO, CdS, WO_3, and TiO_2, have been

[a]*Earth and Environmental Sciences, Bahria University, Islamabad 44000, Pakistan. E-mail: naseem@uspcase.nust.edu.pk; Tel: +925190855281*

[b]*U.S.-Pakistan Center for Advanced Studies in Energy (USPCAS–E), National University of Sciences and Technology (NUST), Islamabad 44000, Pakistan*

[c]*School of Chemical and Materials Engineering (SCME), National University of Sciences and Technology, Islamabad, Pakistan*

utilized as photocatalysts in the production of biodiesel from a wide range of oils.[17–19] TiO_2 nanoparticles have been a center of attraction for photocatalyst applications due to its non-toxicity, chemical stability, large surface area and less production cost. Graphitic carbon nitrides have also emerged as carbon nano materials for wide range of applications including photocatalyst due to their low-cost synthesis, high stability and good optical properties.

Here in this study, novel improved semiconductor-based photocatalyst TiO_2/g-C_3N_4 composite was synthesized and characterized for their structural, morphological, and optical properties and it was utilized to carry out the transesterification reaction of WCO, which resulted in the cleaner production of biodiesel. Optimized reaction parameters were chosen for transesterification reaction under the photocatalytic condition. FTIR was used to characterize the synthesized biodiesel, and other fuel characteristics such as density, viscosity, flashpoint, acid value, and pH were also evaluated and compared with fuel standards. The improved reaction catalyst resulted in an 89.5% yield, and other fuel characteristics were determined to comply with ASTM requirements, indicating that TiO_2/g-C_3N_4 is a promising candidate for biodiesel synthesis. This work shows the potential of cheap semiconductor-based photo-catalyst for biodiesel production using waste cooking oil as a cheaper feedstock for clean energy production.

2. Experimental

2.1. Materials and chemical reagents

Waste cooking oil was gathered from small eateries in nearby areas. Precursors utilized in the synthesis of TiO_2 and g-C_3N_4 are titanium(IV) oxide (Sigma Aldrich, ≥99%, CAS number 12188-41-9) and melamine (Sigma Aldrich, ≥99%, CAS number 108-78-1). Methanol (analytical grade, 99%), ethanol (analytical grade, 99%), concentrated sulfuric acid (analytical grade, 99%), and deionized water (DI) are used as solvents for synthesis, esterification, and transesterification processes.

2.2. Photocatalyst synthesis

2.2.1. Synthesis of TiO_2 nanoparticles. The titanium dioxide nanoparticles were prepared by using the precipitation method, which involved mixing 60 g titania powder with 400 ml of distilled water and stirring constantly at 800 rpm for 24 hours. Then it was allowed to settle down for 12 hours. After that, it was oven dried for 12 hours at 100 °C and then calcined for 6 hours at 500 °C.[20]

2.2.2. Synthesis of graphitic carbon nitride (g-C_3N_4). For the preparation of (g-C_3N_4) melamine was utilized as a precursor, in an alumina crucible 10 g of melamine powder was evenly spread and it was then placed in a muffle furnace for calcination at 550 °C. The yellow powder that was obtained after 4 hours of ramping at 2.5 °C min^{-1} was g-C_3N_4.[21]

2.2.3. Synthesis of TiO_2/g-C_3N_4 composite. Synthesis of titanium dioxide and graphitic carbon nitride composite was done by the wet-impregnation method. Initially, TiO_2 nanoparticles and g-C_3N_4 (wt%) were mixed in a beaker containing 40 ml methanol and ultrasonicated for about 30 minutes for uniform dispersion, after that the subsequent solution was then agitated constantly and heated to 80 °C for 3 hours at 600 rpm to evaporate the solvent. After volatilization of the methanol, the TiO_2/g-C_3N_4 composite was sintered at 300 °C for 2 hours in a box furnace. The synthesized photocatalysts were labeled as TiO_2/g-C_3N_4 (10, 20, and 30 wt%).

2.3. Photocatalyst characterization

The photocatalyst crystal structure was investigated by using the X-ray diffraction (Bruker D8 Advance (Cu-kα)) the morphology and elemental composition were revealed using scanning electron microscopy (VEGA 3LMU, TESCAN), for thermogravimetric analysis (DTG-60/60H) is used to analyze thermal degradations of the synthesized photocatalyst. To analyze the optical properties of synthesized photocatalyst is observed under UV-visible light spectrum by PerkinElmer Lambda 900 Ultraviolet Spectrophotometer.

2.4. Biodiesel production

To generate biodiesel, a two-step method, comprising esterification and transesterification, was employed. Esterification was employed before transesterification to reduce the high FFA concentration in WCO which might promote unwanted saponification during transesterification.

2.4.1. Esterification. For esterification reaction, 100 ml of waste cooking oil and 60 ml ethanol (3% sulphuric acid) was mixed at 55 °C for 3 h at 300 rpm. The resulting mixture was settled down and the oil layer was separated and heated to remove excess ethanol, after which the oil was washed three times with water and oven-dried at 100 °C for two hours to remove excess.[22]

2.4.2. Optimized of reaction conditions. The catalytic activity of prepared photocatalyst TiO_2/g-C_3N_4 (10%, 20%, and 30%) with different catalyst concentrations (1, 2, and 3%) were individually analyzed for transesterification reaction using oil to methanol ratio 1 : 9, reaction time 60 min, reaction temperature 60 °C. The reactions were carried out under solar irradiation at the U.S. Pakistan center for advanced studies in energy, National University of Science and Technology, NUST within the longitudes and latitudes 33.642319°E, 72.98451°N in Islamabad Capital Territory, Pakistan with the reaction mixture being exposed to sunlight between 11:00–13:00 Hrs of the day.

2.4.3. Transesterification of waste cooking oil. The transesterification reaction was then carried out using the esterified oil. First, all the methanol and catalyst (TiO_2/g-C_3N_4) are mixed to form methoxide. After that, the pre-heated waste cooking oil (WCO) 50 ml was added to the beaker containing methoxide, and flux the mixture was agitated for 1 hour at 60 °C at 500 RPMs. Using a separating funnel, the mixture was separated into biodiesel and glycerol when the reaction period was complete. To remove the spent catalyst, the biodiesel was washed three times with water.

2.4.4. Biodiesel yield analysis. The following formula was used to compute the biodiesel yield eqn (1).[7]

$$\text{Yield } \% = \left[\frac{\text{amount of biodiesel produced}}{\text{amount of oil}}\right] \times 100 \qquad (1)$$

2.4.5. Biodiesel characterization. Several variables and techniques were used, including FTIR, pH, flashpoint, kinematic viscosity, relative density, and acid value. The flashpoint of the biodiesel sample was evaluated using a flash point tester (Seta flash series 3 active cool small-scale) (UK). Fourier transform infrared spectroscopy (Cary 630) to analyze the functional group present in produced biodiesel and conventional diesel. A wavelength range of 600 to 4000 cm^{-1} was used to scan the IR spectra. The viscosity of WCO biodiesel was determined using Brookfield DV2T viscometer.

3. Results and discussion

XRD analysis of titanium dioxide nanoparticles, g-C_3N_4, and the composite of TiO_2/g-C_3N_4 (10, 20 and 30%) was performed to determine the crystalline phase of the synthesized photocatalysts. Fig. 1(a) reveals the XRD patterns of TiO_2 nanoparticles and pure g-C_3N_4, main diffraction peaks of TiO_2 nanoparticles that appears at $2\theta = 25.304°$, 36.945°, 37.804°, 38.501°, 48.054°, 53.067°, 55.133°, 62.171°, 62.724°, 68.78°, 70.314°, 74.035°, 75.41°, and (76.104°) which corresponds to (101), (103), (004), (112), (200), (105), (211), (204), (116), (220), (107), (215), and (301) diffraction planes of tetragonal anatase TiO_2 (JCPDS card no. 21-1272) respectively. Two main characteristics peaks were found in pure g-C_3N_4 at about $2\theta = 13.14°$ and 27.57° which corresponds to (100) and (002) diffraction planes of hexagonal graphitic carbon nitride (JCPDS # 87-1526). Fig. 1(b) shows typical diffraction peaks of titanium dioxide and graphitic carbon nitride in TiO_2/10% g-C_3N_4, TiO_2/20% g-C_3N_4, and TiO_2/30% g-C_3N_4 composite. Fig. 1(c) shows the increasing trend of the composition of g-C_3N_4 in composites. The diffraction peaks of g-C_3N_4 increased dramatically with the addition of 30% of g-C_3N_4 in the composite. As a result of the XRD data, several TiO_2/g-C_3N_4 composites were effectively produced. TiO_2 nanoparticles and pure g-C_3N_4 have average crystalline sizes of 28.4 nm and 5.05 nm respectively.

The morphology of the synthesized material was revealed by using scanning electron microscopy. Fig. 2 shows SEM images of TiO_2 nanoparticles, pure g-C_3N_4, and composite TiO_2/g-C_3N_4 (10, 20, and 30%). The SEM images of TiO_2 nanoparticles (a and b) and g-C_3N_4 (c) revealed an agglomeration of small spherical-like nanoparticles and stacked sheet-like structures. Similarly, the SEM image of composite (d–f) TiO_2/g-C_3N_4 (10, 20 and 30%) showed that agglomerate TiO_2 nanoparticles were attached on a sheet-like structure, the composite shows larger porosity indicates the higher number of catalytic sites. The elemental composition of the produced sample was determined using EDS. Table 1 shows the elemental composition of TiO_2, g-C_3N_4, and their respective composites.

The thermal stability of the produced photocatalyst was investigated using TGA. Fig. 3(a and b) shows the TGA curves of TiO_2 nanoparticles, g-C_3N_4, and composite TiO_2/g-C_3N_4 (10, 20, and 30%). Throughout the whole temperature range (0–800 °C),

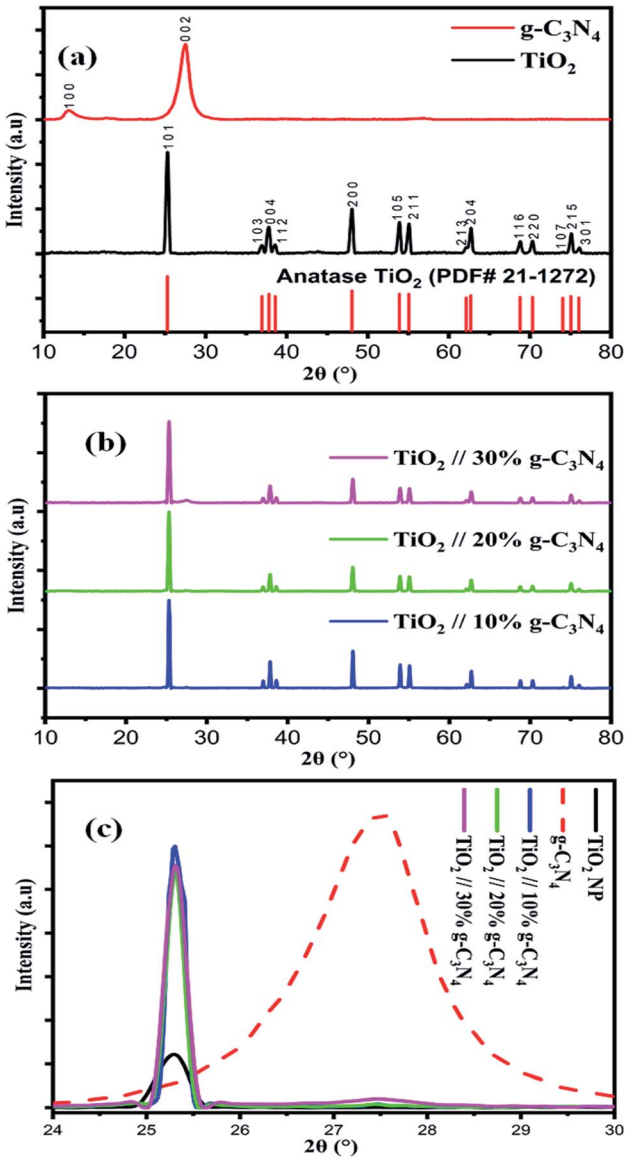

Fig. 1 XRD spectrum of (a) TiO_2 nanoparticles and g-C_3N_4 (b) composite TiO_2/g-C_3N_4 (10, 20 and 30%), (c) trend of g-C_3N_4 in composites.

the TGA curve of TiO_2 nanoparticles shows no weight change. Similarly, at roughly 200 °C, the TGA curve of g-C_3N_4 loses 5 wt% weight, which has been attributed to the elimination of absorbed water. Following that, a rapid mass loss from 600 to 800 °C indicated the loss of tri-*s*-triazine-based units, which were decomposed at around 800 °C. TGA curve of composite TiO_2/g-C_3N_4 (10, 20 and 30%) shows the sharp weight loses at 600 to 800 °C, and the mass loss was 10%, 18%, and 36% respectively, this is due to the decomposition of g-C_3N_4 at these temperatures, which also corresponds to the weight percentage of g-C_3N in the corresponding composite material.

UV-vis was used to investigate the optical properties of the materials; absorption spectra were obtained and the bandgap of prepared photocatalysts was calculated by using Tauc plot. It can be observed in Fig. 3(d) that the TiO_2 nanoparticles absorb

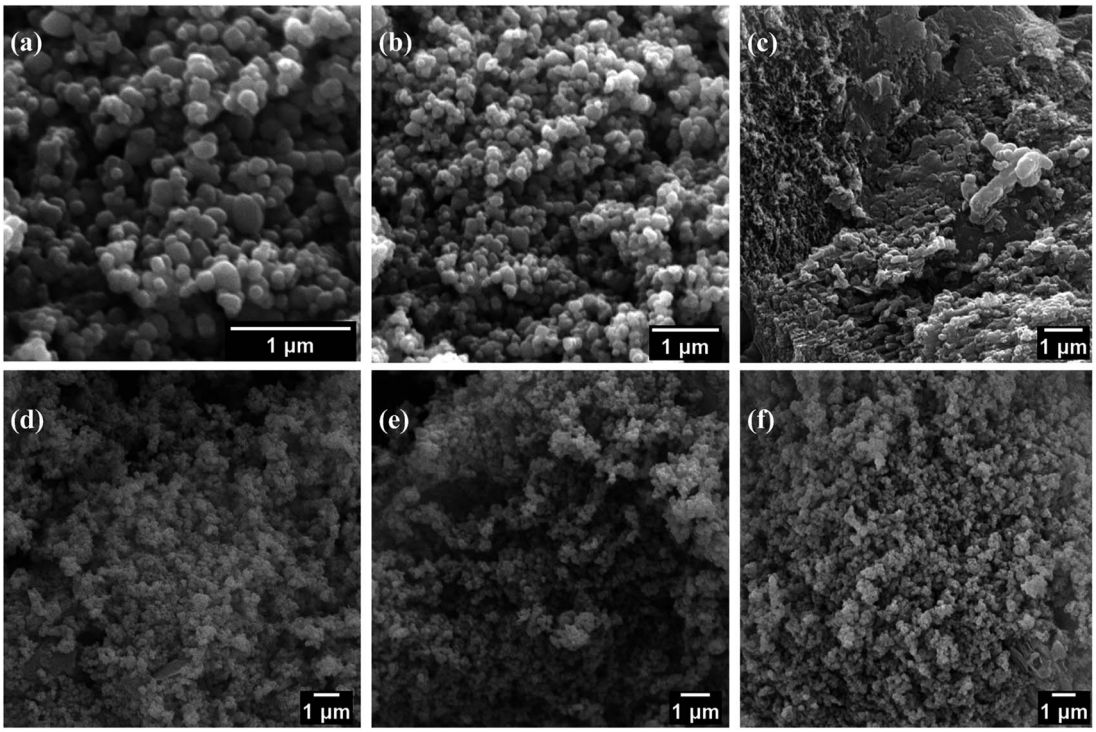

Fig. 2 SEM images of (a and b) TiO_2 nanoparticles (c) pure g-C_3N_4, (d) TiO_2/10% g-C_3N_4, (e) TiO_2/20% g-C_3N_4, and (f) TiO_2/30% g-C_3N_4 composites.

ultraviolet strongly from 200 nm to 400 nm with less absorbance of visible light, UV-vis Spectra of the synthesized composite materials shows the sharp peak ranging in between the 270–285 nm can be associated with $\pi \rightarrow \pi^*$ transition with the C and N centers of g-C_3N_4 linked as a composite material with TiO_2, where N atoms are treated as an n-dopant type in g-C_3N_4, thus the in composite material this band is most likely to related to the appearance of free electron conduction in g-C_3N_4 unit and within TiO_2 nanoparticles and 2D sheets of g-C_3N_4. The UV-vis in between 200 nm to 400 nm of pristine TiO_2 and composite material is showing typical semiconductor absorption behavior which can be ascribed to the charge transfer response of TiO_2 and g-C_3N_4 from valence to the conduction band. Accordingly, the (Tauc plot) of $(\alpha h\nu)^2$ *versus* energy (eV) are shown in Fig. 3(c), corresponding bandgap energies of TiO_2 nanoparticles and composites TiO_2/g-C_3N_4 (10%, 20% and 30%) were estimated to be 3.27, 3.15 3.05 and 2.94 eV respectively. The resulting narrow bandgap of the composite TiO_2/g-C_3N_4 shows that the band gap of TiO_2 was found to be lowered by the addition respective wt% of g-C_3N_4. The conduction band edge of graphitic carbon nitride (g-C_3N_4) is higher than that of TiO_2, which prevents the photogenerated electron–hole pairs from recombination during photocatalytic processes. Therefore, graphitic carbon nitride was used as an efficient co-catalyst photocatalyst to improve the photocatalytic activity of the TiO_2.[23]

The waste cooking oil collected from eateries was firstly filtered to remove any particulate matter and then was heated to 80 °C to remove any water content present in the oil, then it is characterized based on certain physical properties including FFA content, density, and viscosity of the oil. Table 2 shows the physical properties of collected waste cooking oil before its conversion to biodiesel are mentioned. Transesterification reaction occurs when oil FFA content is less than 3%, thus WCO oil is acid esterified and the FFA level is reduced down to less than 3 percent, then transesterification is performed with varied catalyst concentrations.

Table 1 Elemental composition of TiO_2 nanoparticles, g-C_3N_4, and of composite TiO_2/g-C_3N_4 (10, 20 and 30%)

	TiO_2	GCN	TiO_2/g-C_3N_4 (10%)	TiO_2/g-C_3N_4 (20%)	TiO_2/g-C_3N_4 (30%)
	Weight%	Weight%	Weight%	Weight%	Weight%
Ti	63.15		37.29	37.41	17.25
O	36.85		53.49	43.99	40.29
C		63.4	7.11	15.28	35.99
N		36.6	2.11	3.32	6.47

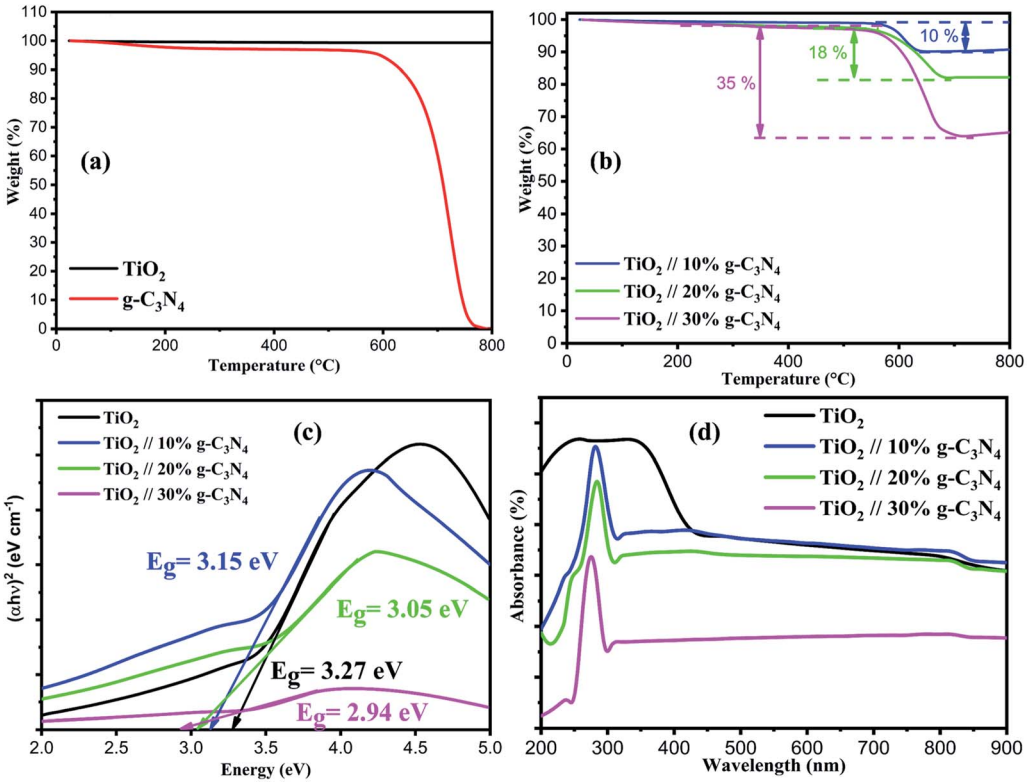

Fig. 3 Represents the TGA curve of (a) TiO_2 and g-C_3N_4 (b) composite TiO_2/g-C_3N_4 (10, 20 and 30%) and UV-visible absorption spectra of (c) Tauc plot used to determine the energy bandgap of the photocatalysts (d) TiO_2, and of composites TiO_2/g-C_3N_4 (10%, 20%, and 30%).

The amount of biodiesel produced as compared with the amount of feedstock used mainly depends on the catalyst used. Therefore, the effect of three different catalyst concentration TiO_2/10% g-C_3N_4 (1, 2 and 3%), TiO_2/20% g-C_3N_4 (1, 2 and 3%) and TiO_2/30% g-C_3N_4 (1, 2 and 3%) on the yield of biodiesel was studied. Out of them the composite TiO_2/g-C_3N_4 (30%) gives no or very less yield (*i.e.*, <10%) because of the congealing temperature is lower than conventional biodiesel, which is why it becomes a jelly-like substance within a fraction of minutes. The obtained results for TiO_2/10% g-C_3N_4 (1, 2 and 3%) and TiO_2/20% g-C_3N_4 (1, 2 and 3%) catalysts show the biodiesel yield of 65%, 70%, 74%, 78%, 89.5% and 68% respectively. It can be seen that product yield varies depending on catalyst concentration. According to the data, the biodiesel yield of 65% was found to be lowest at a catalyst concentration of TiO_2/10% g-C_3N_4 (1% w/w) of oil. The highest biodiesel production of 89.5% was found at a catalyst concentration of TiO_2/20% g-C_3N_4 (2% w/w), which was related to an increase in catalytic sites participating in WCO transesterification processes, and afterward, the yield declined.

The surface functional group of the produced biodiesel by WCO using synthesized TiO_2 and its composites used in different wt% ratio and conventional diesel were identified *via* FTIR was shown in Fig. 4(a and b). In the region of 650 cm^{-1} to 4000 cm^{-1}, the FTIR spectra were examined. Biodiesel's absorption peak was discovered at 3466.83 cm^{-1}, which corresponds to the bending of O–H bonds in alkyl esters. The alkane cluster C–H is stretched unevenly in the strong band at 2850.87 cm^{-1}. At 1740.71 cm^{-1}, the oxygen functional group in biodiesel was identified as symmetrical carbonyl group C=O. The aromatic cluster C–H stretching vibrations are assigned to the band at 1455.57 cm^{-1}. The presence of oxygen components

Table 2 Properties of waste cooking oil and biodiesel produced by using waste cooking oil (WCO) and catalyst

Properties	Waste cooking oil	Bio-diesel produced (using TiO_2/g-C_3N_4 20% (2%))	Standard limit
FFA content (wt% of oil)	10		<3 for transesterification
pH	6.2	7.1	7–9
Flash point (°C)		110	93 (ASTM D93)
Viscosity ($mm^2\ s^{-1}$)	3.38	4.65	1.9–6.0 (ASTM D445)
Acid value (mg $KOH^{-1}\ g^{-1}$)		0.5	0.5 (ASTM D664)
Density (kg m^{-3})	911	890	860–900 (EN ISO 3675)

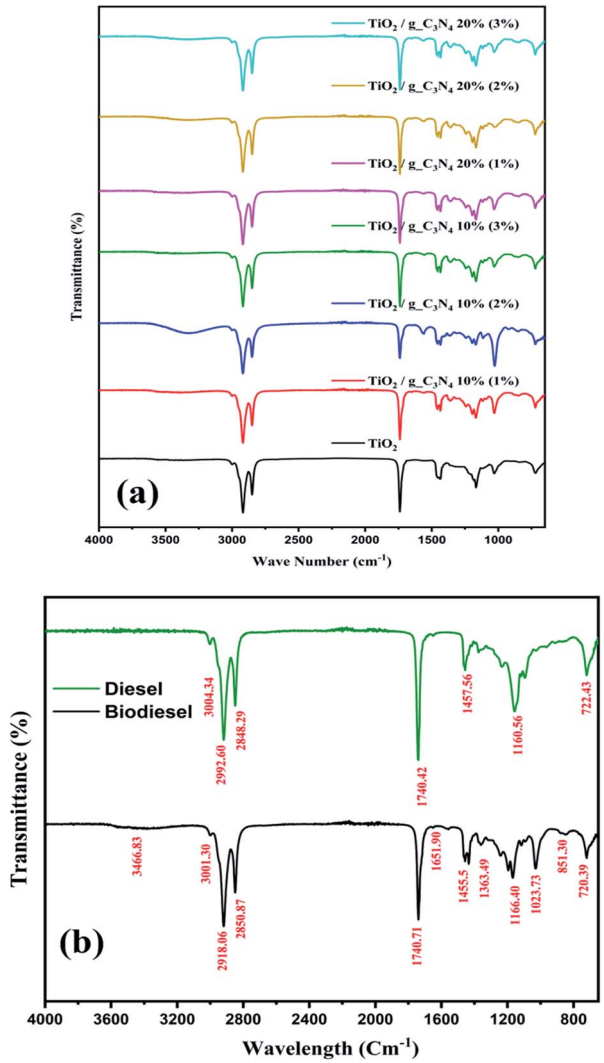

Fig. 4 FTIR spectrum of (a) biodiesel produced by different catalysts by using different catalyst concentrations and (b) WCO biodiesel and conventional diesel.

in biodiesel provides cleaner and complete combustion, unlike conventional diesel. A mixture of bending and stretching aromatic compounds C–H is responsible for the remaining peaks at 1023.73 and 851.30 cm^{-1}. The absorption peak at 1651.90, 1363.49, and 720.39 cm^{-1} confirms the presence of long-chain fatty acids in biodiesel. The regular diesel's spectrum resembled that of biodiesel in parts, particularly in the 3000–2850 cm^{-1} range. A little C=O vibration was also identified at 1740.42 cm^{-1}. The peak in the region from 1740–1750 cm^{-1} is for diesel.

The fuel properties of produced biodiesel such as pH, flash point, kinematic viscosity, relative density, acid number were compared with standards represented in Table 2. The pH value of biodiesel must be taken into consideration. The pH of waste cooking oil biodiesel is neither acidic nor basic. The pH value of biodiesel produced by WCO using TiO_2/20% g-C_3N_4 is 7.1 which falls within the ASTM standard limits. The standard value of flashpoint for biodiesel should be 93 °C or above. The higher flashpoint reduces the chance of unexpected fire hazards. The flashpoint of biodiesel produced by WCO using TiO_2/20% g-C_3N_4 having a value of 110 °C that falls within the ASTM standard limits.

The average viscosity of WCO biodiesel was found to be 4.65 $mm^2\ s^{-1}$ using TiO_2/20% g-C_3N_4 when used in 2% concentration. WCO biodiesel has a viscosity that is within ASTM standard limits (1.9–6.0 $mm^2\ s^{-1}$) and characteristics that are substantially equivalent to petro-diesel (1.9–4.1 $mm^2\ s^{-1}$). The amount of free fatty acids is measured by acid numbers. Oil hydrolysis produces considerable free fatty acids when the acid level is high. The higher the acid number, the lower the oil quality. The acid value of biodiesel produced by WCO using TiO_2/20% g-C_3N_4 was found to be 0.50 mg $KOH^{-1}\ g^{-1}$. The average density of biodiesel produced by WCO using TiO_2/20% g-C_3N_4 was found to be 890 kg m^{-3}. Our findings support the findings of,[22] which found that the density of waste oil (850 kg m^{-3}) was more than petro diesel.

The photocatalyst TiO_2/g-C_3N_4 composite was successfully synthesized for biodiesel production from WCO. The detailed characterization of the prepared photocatalyst (TiO_2/10% g-C_3N_4 and TiO_2/20% g-C_3N_4) was carried out, in which XRD indicates the formation of anatase TiO_2 nanoparticles and g-C_3N_4 with crystal sizes of 28.4 nm and 5.05 nm respectively, SEM images of the composite TiO_2/g-C_3N_4 shows larger porosity, which indicates the higher number of catalytic sites, the thermal stability of the composites TiO_2/g-C_3N_4 (10, 20 and 30%) shows that have great stability against high temperature. UV-vis analysis shows the decreasing bandgaps of 3.27 eV, 3.15 eV, 3.05 eV, and 2.94 eV of TiO_2 nanoparticles with the addition of g-C_3N_4, in 10%, 20%, and 30% concentration. The synthesized photocatalyst was then employed for biodiesel production from WCO. For transesterification with different catalysts TiO_2/g-C_3N_4 (10, 20 & 30%) with different catalysts concentrations (1, 2 and 3%) was experimented. The highest FAME yield (89.5%) was achieved when TiO_2/20% g-C_3N_4, 2% catalyst concentration was used as compared to other catalyst concentrations. The FTIR analysis of WCO biodiesel confirms the presence of specific characteristic peaks as compared with

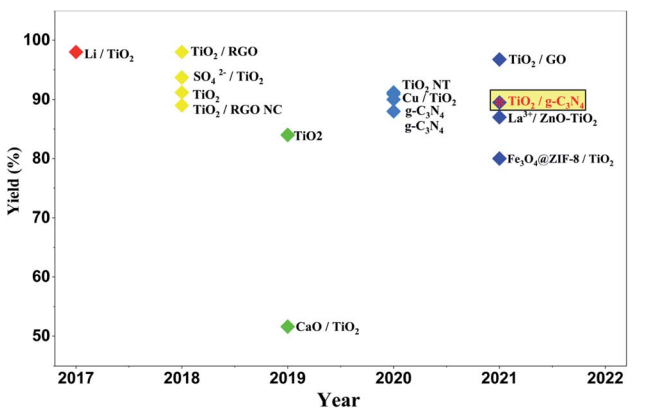

Fig. 5 Represent the recent catalyst yields of similar catalysts used for biodiesel production for transesterification.

Table 3 Comparison of similar catalysts used for transesterification

	Feed stock oil	Catalyst	Oil to methanol ratio	Temperature (°C)	Time (min)	Yield (%)	Ref.
1	WCO	TiO_2/g-C_3N_4	1 : 09	60	60	84.9	This work
2	Waste olive oil	TiO_2	1 : 12	120	240	91.2	24
3	Kemiri sunan oil	TiO_2	1 : 15	60	90	84	25
4	Waste cooking olive oil	TiO_2 NT	1 : 08	65	180	91.2	26
5	WCO	TiO_2/RGO	1 : 12	65	180	98	27
6	WCO	TiO_2/RGO nano composite	1 : 08	65	60	89	28
7	Palm oil	TiO_2-GO	1 : 09	70	40	96.73	29
8	Canola oil	Li/TiO_2	1 : 24	55	90	98	30
9	Palm oil	Cu/TiO_2	1 : 20	45	45	90.93	31
10	Microalgae biomass	CaO/TiO_2	1 : 08	55	120	51.6	32
11	*Jatropha curcas* L. seed oil	SO_4^{2-}/TiO_2	1 : 08	65	60	93.7	33
12	Canola oil	g-C_3N_4	1 : 12	60	90	88	34
13	Canola oil	g-C_3N_4	1 : 24	150	180	90	35
14	WCO	La^{3+}/ZnO–TiO_2	1 : 12	65	180	87	35
15	WFO	Fe_3O_4@ZIF-8/TiO_2	1 : 30	50	65	80	2

regular petro-diesel. Other fuel properties of WCO biodiesel such as density, viscosity, flashpoint, acid value, and pH, were tested, their values are found in good agreement with certain fuel standards. Hence the outcomes of this study reveal that the photocatalytic efficiency of composite TiO_2/g-C_3N_4 for the synthesis of biodiesel from waste cooking oil is greatly improved. Fig. 5 and Table 3 represent a study comparison of this study with recent work done in the domain of TiO_2 based photocatalyst for the transesterification process, which ultimately shows that the TiO_2/g-C_3N_4 (20%) when used in 2% concentration for transesterification yields the biodiesel up to 89.5% has a certain advantage over the certain parameters including oil to methanol ratio, reaction time and temperature when compared with recent work done using similar catalysts, which indicated the higher photocatalytic activity of TiO_2/g-C_3N_4 (20%) due to which the transesterification reaction is faster and requires less reaction temperature and use of methanol is in moderate quantity which indicates that the catalyst is performing well under photocatalytic conditions to convert the maximum quantity of oil to biodiesel. The composite TiO_2/g-C_3N_4 can be used to produce low-cost biodiesel from low-cost feedstocks (WCO) for sustainable energy.

4. Conclusions

The photocatalyst TiO_2/g-C_3N_4 composite was synthesized and employed in the transesterification reaction of waste cooking oil into biodiesel. Under optimum reaction conditions of 60 °C using oil to methanol ratio of 1 : 9, and 1 hour of reaction under sunlight, maximum biodiesel conversion of 89.5% using the catalyst concentration of TiO_2/20% g-C_3N_4, 2 wt% was achieved. Biodiesel produced was characterized by the FTIR technique and its fuel properties were found to be within standards. Biodiesel may be made from cheap feedstocks using semiconductor based photocatalyst TiO_2/g-C_3N_4 (20%) photocatalysts, lowering the cost of the fuel and reducing environmental issues.

Author contributions

M. K. (MS Student) conducted the research and investigation process and wrote the original draft, H. F. (Senior Associate Professor) supervised the student, N. I. (Professor) supervised the student and revised the manuscript, T. N. (Associate Professor) supervised the student, M. Z. B. A. (MS Student) assisted in completing characterization results and experimentation, S. S. E. B. (MS Student) participated across the entire investigation.

Conflicts of interest

There are no conflicts to declare.

Acknowledgements

The authors are grateful to U.S-Pakistan Center for Advance Studies in Energy, NUST, Islamabad and Bahria University, Islamabad for providing all the necessities and financial aid to complete the research project.

References

1 R. A. Meena, J. Banu, R. Kannah, K. Yogalakshmi and J. Kumar, Biohythane production from food processing wastes – Challenges and perspectives, *Bioresour. Technol.*, 2020, **298**, 122–449.

2 A. Sabzevar, M. Ghahramaninezhad and M. Shahrak, Enhanced biodiesel production from oleic acid using TiO_2-decorated magnetic ZIF-8 nanocomposite catalyst and its utilization for used frying oil conversion to valuable product, *Fuel*, 2020, **288**, 119–586.

3 M. Hossain, M. Bhuyan, A. Alam and Y. Seo, Biodiesel from hydrolyzed waste cooking oil using a S-ZrO_2/SBA-15 super acid catalyst under sub-critical conditions, *Energies*, 2018, **11**, 212–323.

4 M. Borah, A. Das, V. Das, N. Bhuyan and D. Deka, Transesterification of waste cooking oil for biodiesel production catalyzed by Zn substituted waste egg shell derived CaO nanocatalyst, *Fuel*, 2019, **242**, 345–354.

5 J. Gardy, A. Osatiashtiani, O. Cespedes, A. Hassanpour, X. Lai, A. Lee, K. Wilson and M. Rehan, A magnetically separable SO_4/Fe–Al–TiO_2 solid acid catalyst for biodiesel production from waste cooking oil, *Appl. Catal., B*, 2018, **234**, 268–278.

6 S. Bhatia, R. Gurav, T. Choi, Y. Han, Y. Park, H. Jung, S. Yang, H. Song and Y. Yang, A clean and green approach for odd chain fatty acids production in *Rhodococcus* sp. YHY01 by medium engineering, *Bioresour. Technol.*, 2019, **286**, 121383.

7 M. Harabi, S. Bouguerra, F. Marrakchi, L. Chrysikou, S. Bezergianni and M. Bouaziz, Biodiesel and crude glycerol from waste frying oil: production, characterization and evaluation of biodiesel oxidative stability with diesel blends, *Sustainable*, 2019, **11**, 1937.

8 G. Corro, U. Pal and N. Tellez, Biodiesel production from *Jatropha curcas* crude oil using ZnO/SiO_2 photocatalyst for free fatty acids esterification, *Appl. Catal., B*, 2013, **129**, 39–47.

9 I. Thushari and S. Babel, Sustainable utilization of waste palm oil and sulfonated carbon catalyst derived from coconut meal residue for biodiesel production, *Bioresour. Technol.*, 2018, **248**, 199–203.

10 L. Buchori, D. Ubay and K. Syahidah, Biodiesel production from waste cooking oil purified with activated charcoal of Salak peel, *Reaktor*, 2018, **18**, 149–154.

11 S. Bhatia, R. Gurav, T. Choi, Y. Han, Y. Park, H. Jung, S. Yang, H. Song and Y. Yang, Effect of synthetic and food waste-derived volatile fatty acids on lipid accumulation in *Rhodococcus* sp. YHY01 and the properties of produced biodiesel, *Energy Convers. Manage.*, 2019, **192**, 385–395.

12 M. Loizides, X. Loizidou, D. Orthodoxou and D. Petsa, Circular bioeconomy in action: Collection and recycling of domestic used cooking oil through a social, reverse logistics system, *Recycling*, 2019, **4**, 16.

13 S. Keera, S. Sabagh and A. Taman, Transesterification of vegetable oil to biodiesel fuel using alkaline catalyst, *Fuel*, 2011, **1**, 42–47.

14 D. Ackbarali, R. Maharaj, N. Mohamed and V. Harry, Potential of used frying oil in paving material: solution to environmental pollution problem, *Environ. Sci. Pollut. Res.*, 2017, **24**, 12220–12226.

15 D. Thoai, P. Hang and D. Lan, Pre-treatment of waste cooking oil with high free fatty acids content for biodiesel production: an optimization study *via* response surface methodology, *Vietnam J. Chem.*, 2019, **57**, 568–573.

16 M. Li, Y. Zheng, Y. Chen and X. Zhu, Biodiesel production from waste cooking oil using a heterogeneous catalyst from pyrolyzed rice husk, *Bioresour. Technol.*, 2014, **154**, 345–348.

17 M. Rahman, Fundamentals of Semiconductor Photocatalysis, *Concepts Semicond. Photocatal.*, 2019, 1–7.

18 G. Corro, N. Sánchez, U. Pal, S. Cebada, J. Luis and G. Fierro, Solar-irradiation driven biodiesel production using Cr/SiO_2 photocatalyst exploiting cooperative interaction between Cr^{6+} and Cr^{3+} moieties, *Appl. Catal., B*, 2016, **203**, 43–52.

19 A. Olivo, D. Zanardo, E. Ghedini, F. Menegazzo and M. Signoretto, Solar fuels by heterogeneous photocatalysis: from understanding chemical bases to process development, *Chem. Eng.*, 2018, **3**, 32.

20 H. Zhu, D. Chen, D. Yue, Z. Wang and H. Ding, *In situ* synthesis of g-C_3N_4-P25 TiO_2 composite with enhanced visible light photoactivity, *J. Nanopart. Res.*, 2014, **10**, 1–10.

21 H. Liu, Z. Zhang, H. He, X. Wang, J. Zhang, Q. Zhang, Y. Tong, H. Liu, S. Ramakrishna, S. Yan and Y. Long, One-step synthesis heterostructured g-C_3N_4/TiO_2 composite for rapid degradation of pollutants in utilizing visible light, *Nanomaterials*, 2018, **8**, 1–15.

22 J. Marchetti and A. s. Errazu, Esterification of free fatty acids using sulfuric acid as catalyst in the presence of triglycerides, *Biomass Bioenergy*, 2008, **32**, 892–895.

23 T. Isimjan, S. Rasul, M. Alouf, M. Khan, I. Alhowaish and T. Ahmed, Rational design of Pd-TiO_2/g-C_3N_4 heterojunction with enhanced photocatalytic activity through interfacial charge transfer, *Clean Energy*, 2019, **3**(1), 59–68.

24 T. Mihankhah, M. Delnavaz and N. Khaligh, Application of TiO_2 nanoparticles for eco-friendly biodiesel production from waste olive oil, *Int. J. Green Energy*, 2018, **15**, 69–75.

25 A. Redjeki and S. Sukirno, Photocatalytic esterification process for methyl ester synthesis from kemiri sunan oil: a novel approach, *AIP Conf. Proc.*, 2019, **2085**, 020058.

26 N. Khaligh, T. Mihankhah, Z. Shahnavaz, L. Zaharania and M. John, Solar energy and TiO_2 nanotubes: biodiesel production from waste cooking olive oil, *Environ. Prog. Sustainable Energy*, 2021, **40**, e13537.

27 M. Borah, A. Devi, R. Saikia and D. Deka, Biodiesel production from waste cooking oil catalyzed by *in situ* decorated TiO_2 on reduced graphene oxide nanocomposite, *Energy*, 2018, **158**, 881–889.

28 S. Soltani, N. Khanian, T. Choong, N. Asim and Y. Zhao, Microwave-assisted hydrothermal synthesis of sulfonated TiO_2-GO core–shell solid spheres as heterogeneous esterification mesoporous catalyst for biodiesel production, *Energy Convers. Manage.*, 2021, **238**, 114165.

29 A. Alsharifi, H. Znad, S. Hena and M. Ang, Biodiesel production from canola oil using novel Li/TiO_2 as a heterogeneous catalyst prepared *via* impregnation method, *Renewable Energy*, 2017, **114**, 1077–1089.

30 A. De and S. Boxi, Application of Cu impregnated TiO_2 as a heterogeneous nanocatalyst for the production of biodiesel from palm oil, *Fuel*, 2020, **265**, 117019.

31 M. Aghilinategh, M. Barati and M. Hamadanian, Supercritical methanol for one put biodiesel production from chlorella vulgaris microalgae in the presence of CaO/TiO_2 nano-photocatalyst and subcritical water, *Biomass Bioenergy*, 2019, **123**, 34–40.

32 C. Chen, L. Cai, X. Shangguan, L. Li, Y. Hong and G. Wu, Heterogeneous and efficient transesterification of *Jatropha curcas* L. seed oil to produce biodiesel catalysed by nano-sized SO_4^{2-}/TiO_2, *R. Soc. Open Sci.*, 2018, **5**, 30564419.

33 M. Devi, M. Barbhuiya and B. Das, Modified mesoporous graphitic carbon nitride: a novel high-performance heterogeneous base catalyst for transesterification reaction, *Sustainable Energy Fuels*, 2020, **4**, 3537–3545.
34 T. deMedeiros, A. Macina and R. Naccache, Graphitic carbon nitrides: efficient heterogeneous catalysts for biodiesel production, *Nano Energy*, 2020, **78**, 105306.
35 M. Guo, W. Jiang, C. Chen, S. Qu, W. Yi and J. Ding, Process optimization of biodiesel production from waste cooking oil by esterification of free fatty acids using La^{3+}/ZnO-TiO_2 photocatalyst, *Energy Convers. Manage.*, 2020, **229**, 113745.